A Near-Infrared Light-Triggered Nanocarrier with Reversible DNA Valves for Intracellular Controlled Release

*Na Li, Zhengze Yu, Wei Pan, Yaoyao Han, Tingting Zhang, and Bo Tang**

A near-infrared (NIR) light-triggered nanocarrier is developed for intracellular controlled release with good stability, high nuclease resistance, and good biocompatibility. The nanocarrier consists of a gold nanorod core and mesoporous silica shell, capped with reversible single-stranded DNA valves, which are manipulated by switching between the laser on/off states. Upon laser irradiation, the valves of the nanocarrier open and the cargo molecules can be released from the mesopores. When the NIR laser is turned off, the valves close and the nanocarrier stops releasing the cargo molecules. The release amount of the cargo molecules can be controlled precisely by adjusting the irradiation time and the laser on-off cycles. Confocal fluorescence imaging shows that the nanocarrier can be triggered by the laser irradiation and the controlled release can be accomplished in living cells. Moreover, the therapeutic effect toward cancer cells can also be regulated when the chemotherapeutic drug doxorubicin is loaded into the nanocarrier. This novel approach provides an ideal platform for drug delivery by a NIR light-activated mechanism with precise control of area, time, and especially dosage.

1. Introduction

Multifunctional nanocarriers combining several useful properties in a single nanostructure have become one of the dominant strategies in drug delivery systems.[1] The nanocarrier can encapsulate the drugs with high loading amount and efficiency, while simultaneously reducing side effects. Recently, many efforts have been made to develop stimuli-triggered drug carriers that can regulate the release of the loaded drug effectively in response to a given stimulus, such as pH change,[2] temperature change,[3] redox activation,[4] enzymatic activity,[5] competitive binding,[6] and photoirradiation.[7] Among these approaches, light-triggered drug delivery has attracted much attention because it does not rely on changes in specific chemical properties of the environment, which would be expected for intracellular or in vivo applications. A variety of light-responsive nanocarriers have been designed based on ultraviolet light or visible light excitation to liberate the entrapped cargo molecules,[8] which may cause damage to the biological samples and is suitable only for in vitro studies because of its quick attenuation in tissue.[9] As a promising candidate, a near-infrared (NIR) light-triggered nanocarrier brings new opportunities to improve the efficiency for drug delivery due to minimal absorbance and maximum penetration for tissues and organs.

The gold nanorods (AuNRs) have strong absorption in the NIR region and can be employed as the local heat sources when irradiated with an NIR laser through the photothermal effect.[10] Mesoporous silica nanoparticles (MSNs) are considered to be ideal candidates for drug delivery because of their high surface area, tunable size, good biocompatibility, and easy functionalization.[11] Although inorganic materials and organic molecules have been widely used as gatekeepers for MSNs, the utility of the biomolecules as valve provides many advantages, such as good biocompatibility and better cellular uptake. Recently, DNA-capped MSNs as the controlled-release platforms have been intensively studied.[9c,12] Most of these platforms performed well in opening the valve to release the cargo molecules triggered by stimulus. However, the valves were not reversible, which may lead to uncontrollable release after the gates are opened. Therefore, it is highly desirable to develop an on-command delivery system that the valve can be opened and closed at will, which could prevent unexpected release and deliver the cargo molecules accurately.

Herein, we develop a novel NIR light-triggered nanocarrier in which the cargo molecules can be loaded into mesoporous silica coated gold nanorods and then capped with reversible single-stranded DNA valves. The gold nanorods (AuNRs) were prepared and employed as a template to build mesoporous silica shell. The cargo molecules were then loaded into the mesoporous silica shell. The single-stranded DNA was anchored to mesoporous silica shell by amide bonds and the bases of DNA were absorbed on the surface of the silica shell via electrostatic interaction,[12a] resulting in the "off" state of the valves. Upon irradiation with the NIR laser with a wavelength that matches the absorption peak of the nanocarrier, the light will be absorbed and converted into heat through the photothermal effect. The heat will dissipate into the surroundings and destroy the electrostatic interaction

Dr. N. Li, Z. Yu, W. Pan, Y. Han, T. Zhang, Prof. B. Tang
College of Chemistry
Chemical Engineering and Materials Science
Engineering Research Center of Pesticide
and Medicine Intermediate Clean Production
Ministry of Education
Key Laboratory of Molecular and Nano Probes
Ministry of Education
Shandong Normal University
Jinan 250014, P. R. China
E-mail: tangb@sdnu.edu.cn

DOI: 10.1002/adfm.201202564

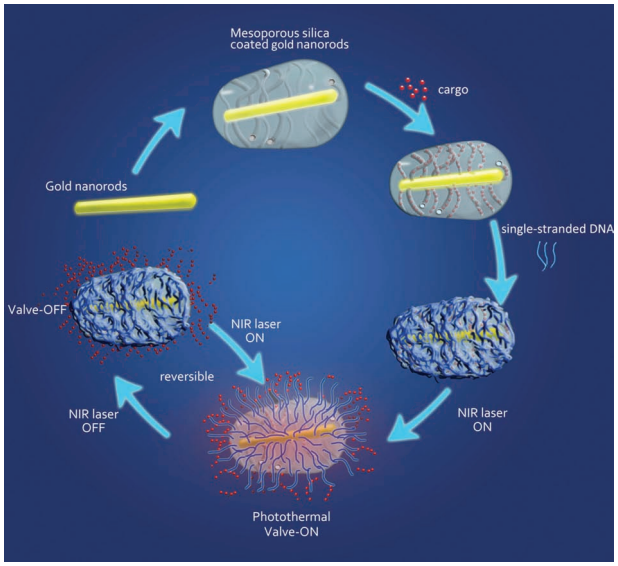

Figure 1. Schematic illustration of the NIR light-triggered nanocarrier with reversible DNA valves for controlled release.

between DNA and silicon shell, leading to the "on" state of the valves and the release of the cargo molecules from the nanocarrier. When the laser is turned off, the heating will immediately stop and the DNA valves will be back to its original state. Then, the nanocarrier stops releasing the cargo molecules. The details of this approach are described in **Figure 1**.

2. Results and Discussion

The AuNRs were typically synthesized using a seed-mediated growth procedure according to a reported protocol with some modifications.[13] As shown in **Figure 2**A, the average length and width of the Au NRs are about 52 and 14 nm, respectively. The modified co-condensation method[14] was employed for the preparation of the amino-functionalized mesoporous silica coated Au NRs (AuNRs@MS-NH_2). As can be seen from Figure 2B, the silica shell of AuNRs@MS-NH_2 is estimated to have a homogeneous thickness of about 22 nm and is composed of disordered mesopores, offering an opportunity for AuNRs@MS-NH_2 to be used as a general drug carrier. N_2 adsorption-desorption isotherms of AuNRs@MS-NH_2 showed a typical Type IV curve with a specific surface area of 137 m^2 g^{-1} and average pore diameter of 2.2 nm with a narrow pore-size distribution (Supporting Information Figure S1). The rhodamine B (RhB) cargo was then loaded in the mesopores of AuNRs@MS-NH_2. Single-stranded DNA (5′-COOH-$(CH_2)_6$-CTCCTGTAATGAAGCGCTAAGTGTAATGG-3′) was used as gatekeeper to cap the pores to prevent the cargo from leaking. The AuNRs@MS-DNA was fabricated through the amidation reaction of AuNRs@MS-NH_2 with carboxyl-functionalized DNA. The morphology of AuNRs@MS-DNA did not show obvious change compared with AuNRs@MS-NH_2 (Figure 2C). The UV-vis absorption spectra of AuNRs, AuNRs@MS-NH_2 and AuNRs@MS-DNA were shown in Figure 2D. The maximum absorption of the Au NRs is at 780 nm and it is red shifted to 805 nm after coating with the silica shell. This is due to the local increase of refractive index and the scattering from the silica shells.[15] After the DNA was modified on the surface of AuNRs@MS-NH_2, the maximum absorption further shifted to 813 nm. Moreover, the appearance of the peak at 260 nm was attributed to the DNA absorbance, indicating the successful modification of DNA on the AuNRs@MS-NH_2 surface. Zeta potential experiments further verified the successful treatment of the nanocarrier in different stages, i.e., –19.3 ± 0.4 mV (AuNRs@MS), 13.1 ± 0.9 mV (AuNRs@MS-NH_2), and –23.1 ± 0.4 mV (AuNRs@MS-DNA).

The stability of the nanocarrier was evaluated by time-dependent fluorescence changes at room temperature. As shown in **Figure 3**A, about 38% RhB was leaked after 168 h for AuNRs@MS-NH_2, while less than 7% RhB was leaked after 168 h for AuNRs@MS-DNA (Figure 3B), indicating that the DNA valves could prevent the cargo molecules from leaking effectively. After the nanocarrier was irradiated with a

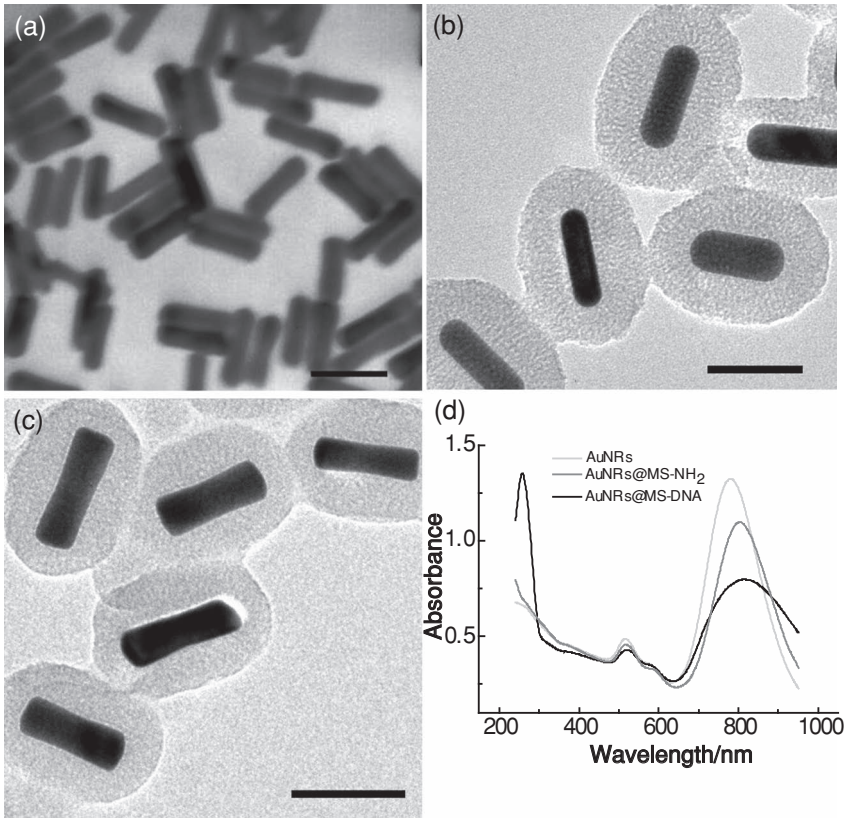

Figure 2. A) TEM image of AuNRs. B) HRTEM image of AuNRs@MS-NH_2. C) HRTEM image of AuNRs@MS-DNA. Scale bars are 50 nm. D) UV-vis spectra of AuNRs, AuNRs@MS-NH_2, and AuNRs@MS-DNA.

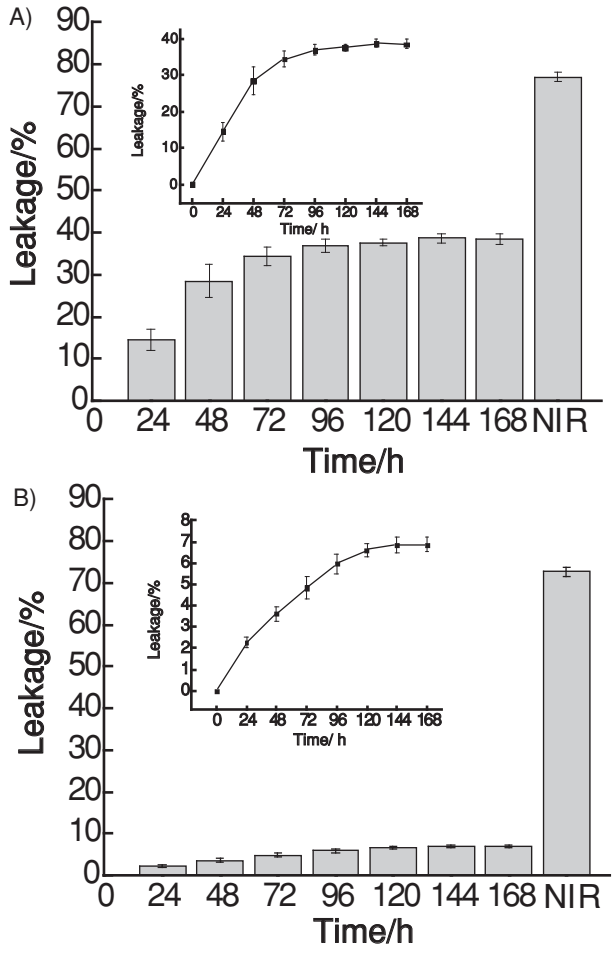

Figure 3. The leakage of the cargo from A) AuNRs@MS-NH_2 (RhB) and B) AuNRs@MS-DNA (RhB) over a time profile at 0, 12, 24, 48, 72, 96, 120, 144, and 168 h, respectively. Then the sample was irradiated with a 808-nm NIR laser for 90 min.

continuous-wave NIR diode laser (808 nm) for 90 min, more than 70% cargo molecules were released, suggesting that the DNA valves could open as expected because of the photothermal effect. To confirm that the release of cargo molecules was indeed induced by the opening of the DNA valves instead of the thermal diffusion upon the NIR irradiation, FAM labeled DNA (5′-CTCCTGTAATGAAGCGCTAAGTGTAATGG-$(CH_2)_6$-FAM-3′) was used as the gatekeeper instead of the carboxylated DNA to cap the pores of AuNRs@MS-NH_2. After being irradiated with the NIR laser, the AuNRs@MS-DNA-FAM solution was centrifuged and the fluorescence intensity of the supernatant was measured. The fluorescence intensity of AuNRs@MS-DNA-FAM without irradiation was used as the control. Supporting Information Figure S2 shows that the fluorescence intensity of irradiated AuNRs@MS-DNA-FAM solution was much higher than that of AuNRs@MS-DNA-FAM without irradiation. This suggests that the electrostatic interaction between DNA and the silicon shell could be destroyed upon irradiation by NIR laser and that the DNA could detach from the surface of the silicon shell. Zeta potential experiments further verified the above results, i.e., –19.0 ± 1.4 mV (AuNRs@MS-DNA-FAM without irradiation after centrifugation) and –7.4 ± 0.9 mV (AuNRs@MS-DNA-FAM with irradiation after centrifugation).

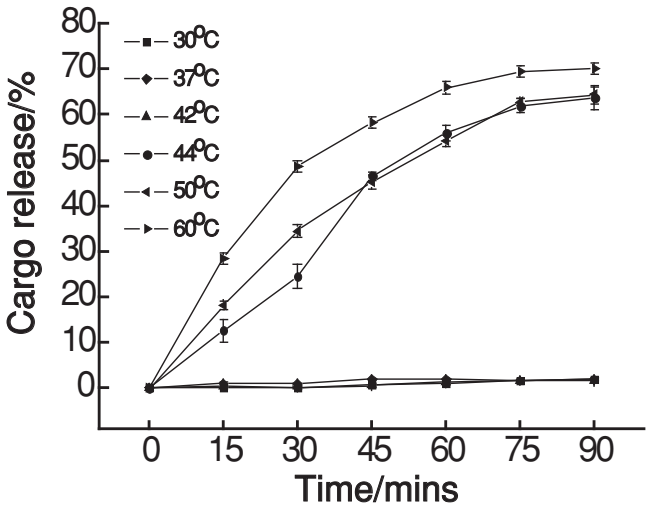

Figure4. The cargo release profiles of AuNRs@MS-DNA (RhB) (0.1 mg/mL) under different temperature (30, 37, 42, 44, 50, and 60 °C).

The effect of temperatures on the opening of the DNA valves of the nanocarrier was also investigated. As shown in **Figure 4**, the release amount of the cargo molecules did not show obvious change when the temperature was lower than 44 °C. This demonstrates that the electrostatic interaction between DNA and the silicon shell still existed and that the DNA valves were closed. When the temperature was ≥44 °C, the release amount of the cargo molecules sharply increased within 90 min, suggesting the opening of the DNA valves.

Prior to applying NIR light as a stimulus to trigger the cargo release, the effect of laser activated temperature increase of the DNA-MS@AuNRs (RhB) solution was investigated under different laser wavelengths and different power densities with increasing irradiation time. **Figure 5** shows that the solution temperature remained unchanged under irradiation at 655 nm

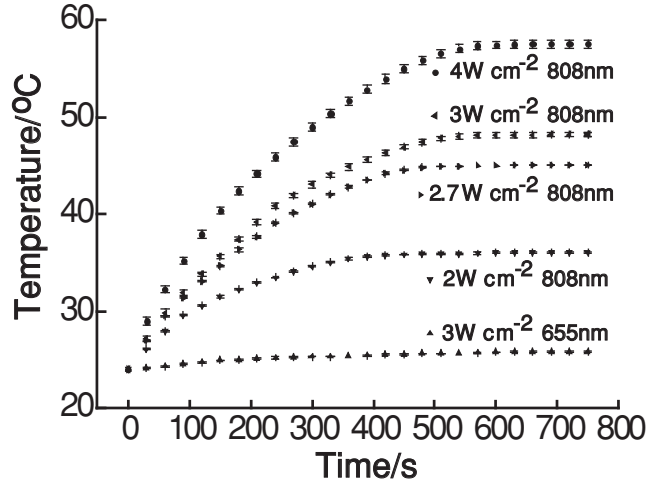

Figure 5. The photothermal effects of the nanocarrier under different laser irradiation.

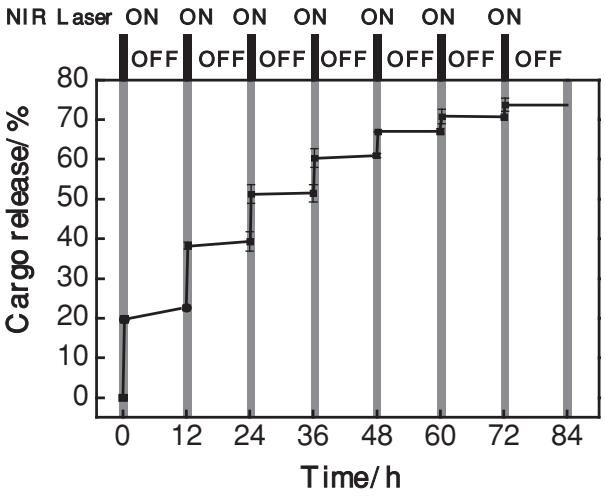

Figure 6. Controlled release profile of AuNRs@MS-DNA (RhB) under NIR laser irradiation (808 nm, 2.7 W·cm^{-2}) for different on/off cycles.

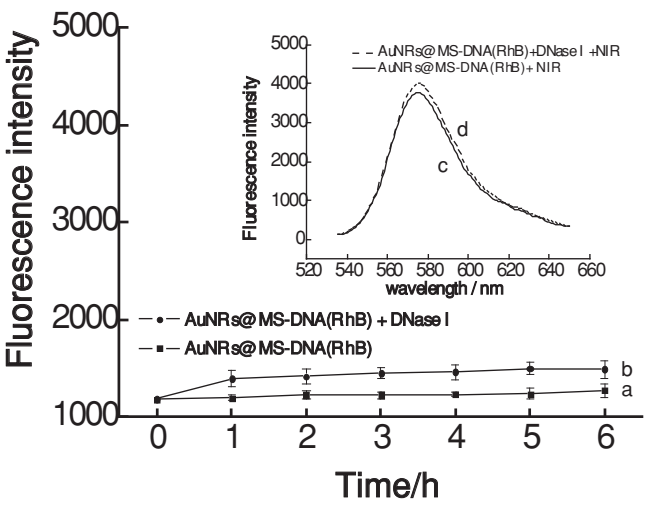

Figure 7. The nuclease stability of AuNRs@MS-DNA(RhB) in the absence or presence of DNase I. Fluorescence curves of AuNRs@MS-DNA(RhB) (0.1 mg/mL) in PBS(10 mM) without DNase I (trace a), in the presence of DNase I (trace b). Inset: Fluorescence spectra the two samples without (trace c) or with (trace d) DNase I after irradiation for 90 min.

(3 W·cm^{-2}) and was of comparable magnitude to the initial temperature. When irradiated with at 808 nm at different power densities, the solution temperature gradually increased up to 500 s, after which the solution temperature remained constant. The final temperature increased with increasing laser power density, i.e., 36 °C for 2 W·cm^{-2}, 45 °C for 2.7 W·cm^{-2}, 48 °C for 3 W·cm^{-2}, and 58 °C for 4 W·cm^{-2}. These results indicate that the nanocarrier was efficiently responsive to the NIR light matched to its absorption peak and the generated photothermal effect was positively correlated with laser power density. In order to open the DNA valves ($T \geq 44$ °C) and minimize the chance of apoptosis by hyperthermia ($T \leq 45$ °C),[12b] a laser power of 2.7 W·cm^{-2} was chosen in the following experiments.

The controlled release of the AuNRs@MS-DNA (RhB) triggered by NIR laser was determined with fluorescence spectroscopic analysis. To evaluate the repeatability and triggered nature of the release, the nanocarrier solutions were manipulated with the NIR laser (808 nm, 2.7 W·cm^{-2}) for several laser on/off cycles. For each cycle, the sample was irradiated for 15 min and then the laser was turned off for 12 h. **Figure 6** shows that the cargo molecules could be released upon irradiation (laser on), indicating the DNA valves were open after irradiation. When the laser was turned off (laser off), the release of the cargo molecules was inhibited, suggesting the DNA valves were close again. The results demonstrated the nanocarrier was reversible after every laser on/off cycle as expected. Approximately 70% RhB was released after seven cycles. When the nanocarrier solution was irradiated by NIR laser continuously, the release amount of cargo was increased with the irradiation time and nearly 70% RhB was released within 100 min (Supporting Information Figure S3). In contrast, about 21% cargo molecules were released upon the first irradiation for 15 min of the AuNRs@MS-NH_2 (RhB) solution and about 20% cargo molecules were still released when the laser was turned off (Supporting Information Figure S4). This indicates that the controlled release could not be achieved for the nanocarrier without the DNA valves. The results show that the current nanocarrier is capable of controlling the cargo release accurately by adjusting the irradiation time and laser on/off states.

The nuclease resistance ability is critical for nanocarriers when used in living cells and this was therefore evaluated under physiological conditions. Enzyme deoxyribonuclease I (DNase I),[16] a common endonuclease, was employed to assess the nuclease stability of the nanocarrier. **Figure 7** showed that the nanocarrier treated with DNase I exhibited slight degradation compared with the case without DNase I. When the nanocarrier only and nanocarrier/DNase I solutions were irradiated with the NIR laser (808 nm) for 90 min, the fluorescence intensities of the two solutions increased greatly (Figure 7, inset). The results indicate the nanocarrier possessed high resistance to nuclease and the release of cargo molecules was indeed due to the irradiation. The nanocarrier could avoid unexpected release of cargo molecules caused by nuclease degradation and it was shown to be viable for application in living cells.

For the application of NIR laser triggered nanocarrier for controlled delivery, intracellular release experiments were carried out in a human breast cancer cell line (MCF-7). As shown in **Figure 8**, nearly no fluorescence signal was observed under confocal laser scanning microscopy when the MCF-7 cells were without irradiation. In order to confirm the controlled release in living cells, three laser on/off cycles were performed in the same cells. For every cycle, the laser on time was chosen to be 10 min to ensure that the final temperature is 45 °C (the irradiation time needs to be more than 8 min, as shown in Figure 5), which makes the DNA valves open and minimizes the potential damage to cells by hyperthermia for a long time. After the first irradiation, a faint fluorescence signal appeared, indicating the successful release of RhB. The fluorescence intensity was gradually enhanced when the laser on/off cycles increased. This demonstrates that the nanocarriers could be triggered by the laser and that the controlled delivery could be achieved in living

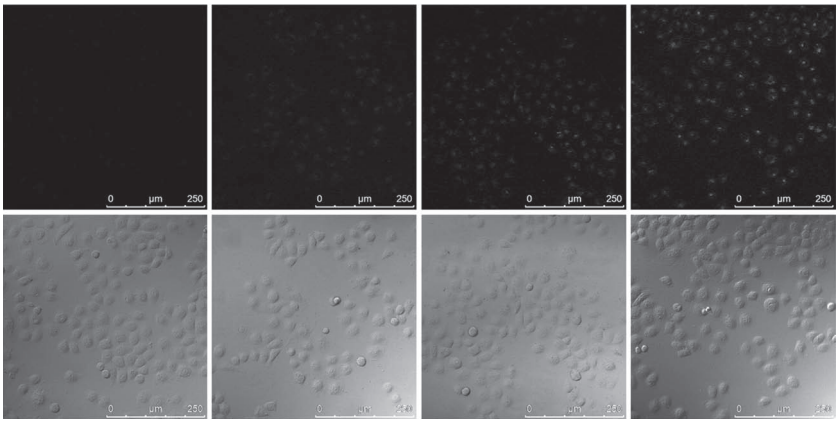

Figure 8. Confocal fluorescence imaging of MCF-7 cells irradiated with NIR laser (808 nm, 2.7 W·cm^{-2}) for different laser on/off cycles.

cells. The bright-field images revealed that the cells were viable throughout the whole imaging experiments of three cycles.

To evaluate the cytotoxicity of the nanocarrier and the photothermal effect by irradiation, an MTT (3-(4, 5-dimethylthiazol-2-yl)-2, 5-diphenylte-trazolium bromide) assay in MCF-7 cells was performed. The absorbance of MTT at 490 nm is dependent on the degree of activation of the cells. The cell viability was expressed by the ratio of absorbance of the treated cells (incubated with the nanocarrier or irradiated with NIR laser) to that of the untreated cells. The results indicated that the nanocarrier showed almost no cytotoxicity or side effects in living cells (**Figure 9**A). The apoptosis induced by irradiation and the photothermal effects was also investigated. Figure 9B indicated that no obvious decrease in the cell viability was observed after each irradiation, which further confirmed, as expected, that the NIR laser with a power density of 2.7 W·cm^{-2} exerted almost no damage on the living cells.

For further application of the nanocarrier, a chemotherapeutic drug doxorubicin (Dox) was loaded to investigate if the therapeutic effect could be controlled using the current nanocarrier. Figure 9C shows that the cell viability is about 95% without the irradiation when the nanocarrier was incubated with the MCF-7 cells, suggesting that the nanocarrier indeed performed well in preventing the Dox molecules from leaking. The cells were then treated with different laser on/off cycles; the cell viability decreased with increasing number of irradiation cycles. After three cycles of irradiation, only about 50% cells survived. The result is consistent with the in vitro release experiment and intracellular imaging, which further confirmed that the release amount of cargo molecules could be controlled using the nanocarrier.

3. Conclusions

We have presented a novel NIR laser-triggered nanocarrier based on mesoporous, silica-coated gold nanorods with reversible DNA valves. The reversible DNA valves of the nanocarrier were manipulated by switching the laser on/off states, which was capable of controlling the release amount of cargo molecules. Moreover, the nanocarrier possesses good stability, high nuclease resistance and good biocompatibility. Intracellular imaging experiments indicated the nanocarrier could be triggered with a NIR laser and the controlled release could be achieved in living cells. When doxorubicin was loaded into the nanocarrier, the therapeutic effect also could be controlled. Compared to the reported nanocarriers, the current approach could deliver the cargo molecules accurately in a controlled manner, which is indispensable for the treatment of some diseases with precise dosage at a desired time in a specified area. We anticipate that the nanocarrier could provide new insights for designing the on-command drug delivery systems.

4. Experimental Section

Materials: DNA oligonucleotides were synthesized and purified by Sangon Biotechnology Co., Ltd (Shanghai, China). 3-(4,5-dimethylthiazol-2-yl)-2,5-diphenyltetrazolium bromide (MTT), doxorubicin (Dox) and rhodamine B (RhB) were purchased from Sigma Chemical Company; deoxyribonuclease I (DNase I) was purchased from Solarbio Science and Technology Co., Ltd. (Beijing, China); sodium borohydride ($NaBH_4$), cetyltrimethyl ammonium bromide (CTAB), silver nitrate ($AgNO_3$), ascorbic acid, tetraethyl orthosilicate (TEOS), and hydrogen tetrachloroaurate (III) ($HAuCl_4{\cdot}4H_2O$) were purchased from China National Pharmaceutical Group Corporation (Shanghai, China); (3-aminopropyl) triethoxysilane (APTES) and 1-ethyl-3-(3-dimethylaminopropyl) carbodiimide hydrochloride (EDC) were purchased from Alfa Aesar Chemical Ltd (Tianjin, China). All the chemicals were of analytical grade and used without further purification. Sartorius ultrapure water (18.2 MΩ cm) was used throughout the experiments. The human breast cancer cell line (MCF-7) was purchased from KeyGEN biotechnology Company (Nanjing, China).

Instruments: Near infrared (NIR) lasers with irradiation wavelength of 655 nm (MLL-III-655) and 808 nm (MDL-III-808) were purchased from Changchun New Industries Optoelectronics Tech. Co., Ltd (Changchun, China). Transmission electron microscopy (TEM) was carried out on a JEM-100CX II electron microscope and high resolution transmission electron microscopy (HRTEM) was carried out on a JEM-2100 electron microscope, respectively. N_2 adsorption-desorption isotherms were recorded on a Micromeritics ASAP2020 surface area and porosity analyzer. The samples were degassed at 150 °C for 5 h. The specific surface areas were calculated from the adsorption data in the low pressure range using the BET model and pore size was determined using the Barrett–Joyner–Halenda (BJH) method. Absorption spectra were measured on a Pharmaspec UV-1700 UV-vis spectrophotometer (Shimadzu, Japan). Fluorescence spectra were obtained with FLS-920 Edinburgh fluorescence spectrometer with a xenon lamp and 1.0 cm quartz cells at the slits of 3.0/3.0 nm. All pH measurements were performed with a pH-3c digital pH-meter (Shanghai LeiCi Device Works, Shanghai, China) with a combined glass-calomel electrode. Absorbance was measured in a microplate reader (RT 6000, Rayto, USA) in the MTT assay. Confocal fluorescence imaging studies were performed with a TCS SP5 confocal laser scanning microscopy (Leica Co., Ltd. Germany) with an objective lens (40×).

Preparation of AuNRs: Gold nanorods (AuNRs) were typically synthesized using a seed-mediated growth procedure according to a reported protocol with some modifications.[13] Seed solution was first synthesized by mixing $HAuCl_4$ (10 mM, 0.25 mL) and CTAB (0.1 M, 10 mL). Next, 0.6 mL ice-cold $NaBH_4$ aqueous solution (0.01 M) was

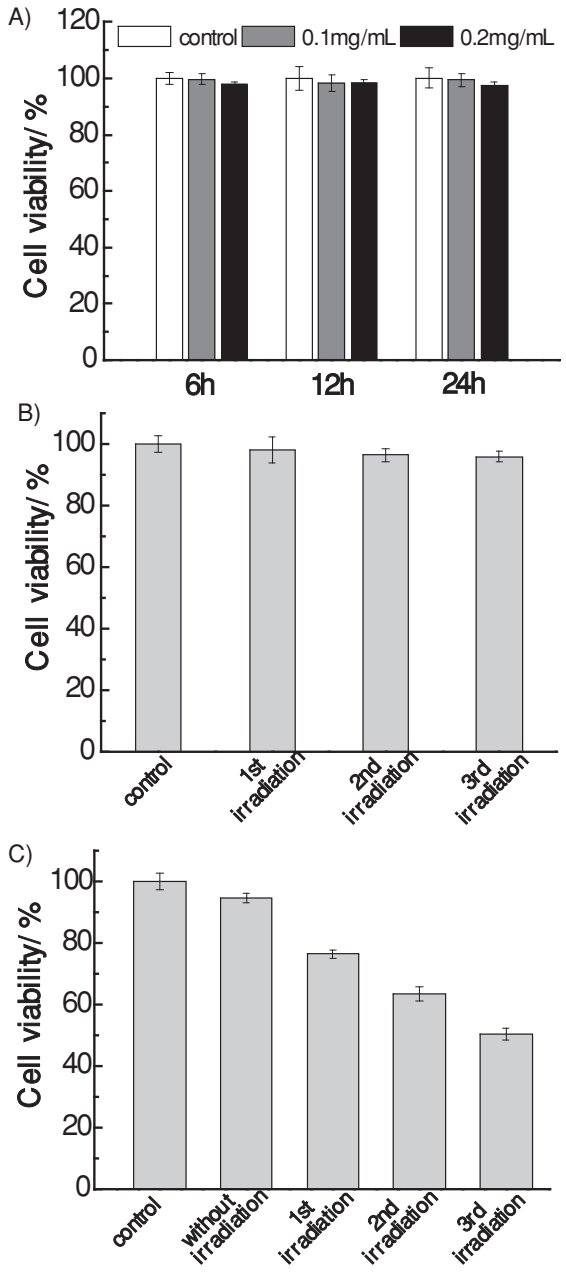

Figure 9. A) Cell viability of MCF-7 cells incubated with different amounts of AuNRs@MS-DNA (0.1 and 0.2 mg/mL) for different times (6, 12, and 24 h). B) Cell viability of MCF-7 cells incubated with AuNRs@MS-DNA for different laser on/off cycles. C) Cell viability of MCF-7 cells incubated with AuNRs@MS-DNA (Dox) for different laser on/off cycles.

added to the mixture which resulted in formation of a bright brownish-yellow solution. This solution was kept at 25 °C at least 2 h. The growth solution was prepared as follows. CTAB (0.1 M, 40 mL) was added to $HAuCl_4$ (10 mM, 2 mL) with gentle stirring. Then, $AgNO_3$ (0.01 M, 320 µL), HCl (1.0 M, 0.8 mL) and ascorbic acid (0.1 M, 0.32 mL) were successively added to the above mixture. Finally, 48 µL seed solution was added to the growth solution and the growth medium was kept at 27 °C for more than 6 h before further use.

Preparation of AuNRs@MS-NH_2: Amino modified mesoporous silica coated AuNRs were synthesized using the typical co-condensation method reported previously with some modifications.[14] The as-synthesized AuNRs were washed by centrifugation at 10 000 rpm for 10 min twice to remove excess CTAB and redispersed in 100 mL water. NaOH (0.1 M, 0.3 mL) was added to the 30 mL prepared AuNRs upon gentle stirring for 10 min, followed by the addition of 45 µL of 20% TEOS in methanol along with 15 µL of 2% APTES in methanol three times under gentle stirring at 30 min intervals. The mixture was reacted for 24 h to form the mesoporous silica shell. The as-synthesized AuNRs@MS-NH_2 was washed with methanol and water for several times to remove the CTAB remained inside the mesopores. The precipitates were finally dispersed in 6 mL water to get a solution with concentration of 0.2 mg/mL. The AuNRs@MS-NH_2 was dried and weighted for further use.

Preparation of AuNRs@MS-DNA (RhB) and AuNRs@MS-DNA (Dox): 2 mL as-prepared AuNRs@MS-NH_2 solution was added to 10 mL RhB solution (0.5 mg/mL). The mixture was stirred for 3 days in darkness to reach the maximum loading. The RhB loaded AuNRs@MS solution was centrifuged (10 000 rpm, 10 min) and washed twice with water to remove the RhB molecules absorbed physically on the outer surface of the silica shell. The precipitates were redispersed in 4 mL MES buffer (10 mM, pH 6.0). AuNRs@MS-DNA was obtained by coupling the carboxl group of the oligonucleotides and the amino group on the surface of AuNRs@MS-NH_2 to form the amido bonds. 17.8 µL EDC (2.8 mM) solution was added to 100 µL of single-stranded DNA (100 µM) solution with the sequence of 5′-COOH-$(CH_2)_6$-ACTCCTGTAATGAAGCGCTAAGTGTAATGG-3′. The solution was mixed and reacted for 30 min at room temperature to activate carboxylate groups. The mixture was then added to 2 mL RhB loaded AuNRs@MS solution with gentle stirring in darkness. The solution was reacted for 24 h which resulted in the formation of the amido bonds. Following this, the precipitates were centrifuged (10 000 rpm, 10 min) and washed with PBS buffer (10 mM, pH 7.4. 100 mM NaCl, 1 mM $MgCl_2$) for three times and finally redispersed in 2 mL PBS buffer. The preparation of AuNRs@MS-DNA (Dox) was same as the method mentioned above.

Quantitation of RhB Loaded into the Nanocarrier: To quantify the RhB loaded into the nanocarrier, 2 mL AuNRs@MS-DNA (RhB) solution was heated in the water bath at 80 °C for 2 h. The sample was centrifuged (10 000 rpm, 10 min) and the supernate was separated. Then, the precipitates were redispersed in 2 mL PBS buffer. The above procedure was repeated at least twice to ensure the RhB release from the pores completely. The fluorescence intensity (λ_{ex} = 532 nm, λ_{em} = 575 nm) of the supernate was measured and the concentrations of RhB were determined according to a standard linear calibration curve of RhB (Supporting Information Figure S5). The loading content of RhB was calculated to be 0.0192 mg RhB per 1 mg AuNRs@MS-NH_2.

Stability of the Nanocarriers: To evaluate the stability of the nanocarrier, the as-prepared 2 mL AuNRs@MS-NH_2 (RhB) or AuNRs@MS-DNA (RhB) (0.1 mg/mL) was stored at room temperature and the fluorescence intensity of the sample was measured (λ_{ex} = 532 nm, λ_{em} = 575 nm) at 0, 24, 48, 72, 96, 120, 144, and 168 h, respectively. After that, this sample was irradiated with NIR laser at 808 nm for 90 min and the fluorescence intensity was also measured. The experiment was repeated three times and the data are shown as the mean ± SD.

Confirmation of the Opening of DNA Valves Upon NIR Laser Irradiation: To confirm that the DNA valves could be open upon the NIR irradiation, FAM labeled DNA (5′-CTCCTGTAATGAAGCGCTAAGTGTAATGG-$(CH_2)_6$-FAM-3′) was used as gatekeeper instead of the carboxylated DNA (5′-COOH-$(CH_2)_6$-CTCCTGTAATGAAGCGCTAAGTGTAATGG-3′) to cap the pores of AuNRs@MS-NH_2. In this case, there was only electrostatic interaction between DNA and the silicon shell and no covalent bond between them, when the electrostatic interaction was destroyed, the DNA would detach from the surface of silicon shell. 100 µL of FAM labeled single-stranded DNA (100 µM) solution was added to 2 mL as-prepared AuNRs@MS-NH_2 solution. The mixture was stirred for 12 h in the darkness to make the DNA absorb on the surface of AuNRs@MS-NH_2 and cap the porous. The mixture was then centrifuged (10 000 rpm, 10 min) and washed with water to remove the excess DNA molecules. The precipitates (AuNRs@MS-DNA-FAM) were finally dispersed in 2 mL PBS buffer. The solution was then divided into two parts. One part (1 mL) was irradiated with the NIR laser (808 nm,

2.7 W·cm^{-2}) for 15 min and the other part was kept without treatment as the control. Both the two samples were kept in the darkness to prevent FAM from photobleaching. The two samples were immediately centrifuged (10 000 rpm, 10 min). The fluorescence intensity of the supernate was measured. The precipitates of each sample were redispersed into 1 mL water. The above procedure was repeated twice to make the DNA molecules desorption from the silicon shell and the control group was also centrifuged twice to keep the consistency principle. Finally, the precipitates of the two samples were redispersed into 1 mL water and the zeta potential was measured. Each experiment was repeated at least three times and the data are shown as the mean ± SD.

Determination of the Critical Temperature of the DNA Valves: To determine the critical temperature of the DNA valves to open, six samples of 2 mL AuNRs@MS-DNA (RhB) (0.1 mg/mL) in PBS buffer were heated in water bath with different temperatures (30, 37, 42, 44, 50, and 60 °C). Each sample was heated for 90 min and the fluorescence intensity was measured every 15 min. The final fluorescence intensity of the dye released completely was measured as mentioned above. The percentage of dye release from the nanocarrier was calculated as follows: (fluorescence intensity of each sample at different time)/(the final fluorescence intensity of the sample). Each experiment was repeated at least three times and the data are shown as the mean ± SD.

Effect of Laser Induced Temperature Change: Five samples of 2 mL AuNRs@MS-DNA (RhB) (0.1 mg/mL) were irradiated under different laser and different power densities. The laser power densityies used were 3.0 W·cm^{-2} at 655 nm, and 2.0, 2.7, 3.0, and 4.0 W·cm^{-2} 808 nm. Each sample was irradiated for 750 s and the temperature was recorded every 30 s. The sample was exposed to the laser light with a beam area of 0.4 cm^2. Each experiment was repeated at least three times and the data are shown as the mean ± SD.

Controlled Release of the Nanocarrier: The release amount of RhB for seven laser on/off cycles was evaluated to study the reversibility of valve on/off cycle and triggered nature of the release. 2 mL AuNRs@MS-NH_2 (RhB) or AuNRs@MS-DNA (RhB) (0.1 mg/mL) in PBS buffer was irradiated with NIR laser (808 nm, 2.7 W·cm^{-2}) for several laser on/off cycles. For each cycle, the sample was first irradiated for 15 min then cooled to room temperature for 15 min and the fluorescence intensity of the sample was measured. The sample was then kept at room temperature for 12 h and the fluorescence intensity of the sample was measured. In addition, to evaluate the relationship of the release amount of cargo and irradiation time, 2 mL AuNRs@MS-DNA (RhB) (0.1 mg/mL) was irradiated with the NIR laser (808 nm, 2.7 W·cm^{-2}) for 105 min continuously. Each experiment was repeated at least three times and the data are shown as the mean ± SD.

Nuclease Assay: Two groups of 2 mL AuNRs@MS-DNA (RhB) (0.1 mg/mL) in PBS buffer were incubated at 37 °C. After allowing the samples to equilibrate (10 min), 1.3 μL of DNase I in assay buffer (2 U/L) was added to one group. The fluorescence signal of the two samples was monitored for 6 h and was collected at intervals during this period. These two groups were then irradiated with the NIR laser (808 nm, 2.7 W·cm^{-2}) for 90 min, and the fluorescence was measured after the solution was cooled to room temperature. The experiment was repeated at least three times and the data are shown as mean ± SD.

Confocal Fluorescence Imaging: MCF-7 cells were cultured on chamber slides for 24 h. The AuNRs@MS-DNA (RhB) (0.1 mg/mL) was delivered into the cells in RPMI-1640 culture medium at 37 °C for 12 h. Cells were then washed twice with PBS buffer and 2 mL RPMI-1640 culture medium was added. The cells were examined with confocal laser scanning microscopy (CLSM) with 543 nm excitation. Next, three NIR laser on/off cycles were performed in the same cells. For each cycle, the cells were irradiated for 10 min then examined by CLSM with 543 nm excitation followed by 2 h incubation.

MTT Assay: MCF-7 cells were cultured in 96-well microtiter plates and incubated at 37 °C in 5% CO_2 for 24 h. MCF-7 cells were incubated with culture medium, AuNRs@MS-DNA (0.1 mg/mL, 0.2 mg/mL) for different times (6, 12, and 24 h), respectively. Next, 150 μL MTT solution (0.5 mg/mL) was added to each well. After 4 h, the remaining MTT solution was removed, and 150 μL of DMSO was added to each well to dissolve the formazan crystals. The absorbance was measured at 490 nm with a RT 6000 microplate reader. (Figure 9A) Then the MCF-7 cells were incubated with culture medium and AuNRs@MS-DNA (0.1 mg/mL) (Figure 9B) or AuNRs@MS-DNA (Dox) (0.1 mg/mL) (Figure 9C) for 12 h. The cells were then irradiated with the NIR laser (808 nm, 2.7 W·cm^{-2}) for different times. Each irradiation time lasted for 10 min at 2 h intervals. After irradiation, the cells were incubated at 37 °C for 24 h. The cells were then treated as mentioned above. Each experiment was repeated at least three times and the data are shown as the mean ± SD.

Supporting Information

Supporting Information is available from the Wiley Online Library or from the author.

Acknowledgements

This work was supported by 973 Program (2013CB933800), National Natural Science Foundation of China (21035003, 21227005, 21105059), Specialized Research Fund for the Doctoral Program of Higher Education of China (20113704130001), Shandong Distinguished Middle-Aged and Young Scientist Encourage and Reward Foundation (BS2011CL037) and Program for Changjiang Scholars and Innovative Research Team in University.

Received: September 6, 2012
Revised: October 26, 2012
Published online: December 2, 2012

[1] a) V. P. Torchilin, *Adv. Drug Delivery Rev.* **2006**, *58*, 1532; b) K. Riehemann, S. W. Schneider, T. A. Luger, B. Godin, M. Ferrari, H. Fuchs, *Angew. Chem. Int. Ed.* **2009**, *48*, 872; c) Z. Li, J. C. Barnes, A. Boscoy, J. F. Stoddart, J. I. Zink, *Chem. Soc. Rev.* **2012**, *41*, 2590.

[2] a) E. Aznar, M. D. Marcos, R. Martinez-Manez, J. Soto, P. Amoros, C. Guillem, *J. Am. Chem. Soc.* **2009**, *131*, 6833; b) R. Liu, Y. Zhang, X. Zhao, A. Agarwal, L. J. Mueller, P. Feng, *J. Am. Chem. Soc.* **2010**, *132*, 1500; c) H. P. Rim, K. H. Min, H. J. Lee, S. Y. Jeong, S. C. Lee, *Angew. Chem. Int. Ed.* **2011**, *50*, 8853.

[3] a) C. R. Thomas, D. P. Ferris, J. H. Lee, E. Choi, M. H. Cho, E. S. Kim, J. Cheon, J. I. Zink, *J. Am. Chem. Soc.* **2010**, *132*, 10623; b) E. Aznar, L. Mondragón, J. V. Ros-Lis, F. Sancenón, M. D. Marcos, R. Martínez-Máñez, J. Soto, E. Pérez-Payá, P. Amorós, *Angew. Chem. Int. Ed.* **2011**, *50*, 11172.

[4] a) C. Y. Lai, B. G. Trewyn, D. M. Jeftinija, K. Jeftinija, S. Xu, S. Jeftinija, V. S. Y. Lin, *J. Am. Chem. Soc.* **2003**, *125*, 4451; b) R. Liu, X. Zhao, T. Wu, P. Feng, *J. Am. Chem. Soc.* **2008**, *130*, 14418.

[5] a) K. Patel, S. Angelos, W. R. Dichtel, A. Coskun, Y. W. Yang, J. I. Zink, J. F. Stoddart, *J. Am. Chem. Soc.* **2008**, *130*, 2382; b) C. Park, H. Kim, S. Kim, C. Kim, *J. Am. Chem. Soc.* **2009**, *131*, 16614; c) A. Bernardos, E. Aznar, M. D. Marcos, R. Martínez-Máñez, F. Sancenón, J. Soto, J. Manuel Barat, P. Amorós, *Angew. Chem. Int. Ed.* **2009**, *48*, 5884; d) P. D. Thornton, A. Heise, *J. Am. Chem. Soc.* **2010**, *132*, 2024.

[6] a) E. Climent, M. D. Marcos, R. Martínez-Máñez, F. Sancenón, J. Soto, K. Rurack, P. Amorós, *Angew. Chem. Int. Ed.* **2009**, *48*, 8519; b) Y. Zhao, B. G. Trewyn, I. I. Slowing, V. S. Y. Lin, *J. Am. Chem. Soc.* **2009**, *131*, 8398.

[7] a) J. L. Vivero-Escoto, I. I. Slowing, C. W. Wu, V. S. Y. Lin, *J. Am. Chem. Soc.* **2009**, *131*, 3462; b) C. Park, K. Lee, C. Kim, *Angew. Chem. Int. Ed.* **2009**, *48*, 1275; c) J. Croissant, J. I. Zink, *J. Am. Chem. Soc.* **2012**, *134*, 7628.

[8] a) Y. Zhu, M. Fujiwara, *Angew. Chem. Int. Ed.* **2007**, *46*, 2241; b) D. P. Ferris, Y. L. Zhao, H. A. Khatib, J. F. Stoddart, J. I. Zink, *J. Am. Chem. Soc.* **2009**, *131*, 1686.

[9] a) A. Schwarz, S. Ständer, M. Böhm, D. Kulms, H. Van Steeg, J. Krutmann, T. Schwarz, *Nat. Cell Biol.* **2002**, *4*, 26; b) M. S. Yavuz, Y. Cheng, J. Chen, C. M. Cobley, Q. Zhang, J. Xie, K. H. Song, A. G. Schwartz, L. V. Wang, Y. Xia, *Nat. Mater.* **2009**, *8*, 935; c) X. Yang, X. Liu, Z. Liu, F. Pu, J. Ren, X. Qu, *Adv. Mater.* **2012**, *24*, 2890.

[10] a) M. C. Daniel, D. Astruc, *Chem. Rev.* **2004**, *104*, 293; b) X. Huang, I. H. El-Sayed, W. Qian, M. A. El-Sayed, *J. Am. Chem. Soc.* **2006**, *128*, 2115; c) M. Hu, J. Chen, Z. Y. Li, L. Au, G. V. Hartland, X. Li, M. Marquez, Y. Xia, *Chem. Soc. Rev.* **2006**, *35*, 1084; d) A. M. Alkilany, L. B. Thompson, S. P. Boulos, P. N. Sisco, C. J. Murphy, *Adv. Drug Delivery Rev.* **2012**, *64*, 190; e) Z. Zhang, L. Wang, J. Wang, X. Jiang, X. Li, Z. Hu, Y. Ji, X. Wu, C. Chen, *Adv. Mater.* **2012**, *24*, 1418.

[11] a) I. I. Slowing, J. L. Vivero-Escoto, C. W. Wu, V. S. Y. Lin, *Adv. Drug Delivery Rev.* **2008**, *60*, 1278; b) Z. Li, J. C. Barnes, A. Bosoy, J. F. Stoddart, J. I. Zink, *Chem. Soc. Rev.* **2012**, *41*, 2590; c) P. Yang, S. Gai, J. Lin, *Chem. Soc. Rev.* **2012**, *41*, 3679.

[12] a) E. Climent, R. Martínez-Máñez, F. Sancenón, M. D. Marcos, J. Soto, A. Maquieira, P. Amorós, *Angew. Chem. Int. Ed.* **2010**, *49*, 7281; b) Y. T. Chang, P. Y. Liao, H. S. Sheu, Y. J. Tseng, F. Y. Cheng, C. S. Yeh, *Adv. Mater.* **2012**, *24*, 3309; c) C. L. Zhu, C. H. Lu, X. Y. Song, H. H. Yang, X. R. Wang, *J. Am. Chem. Soc.* **2011**, *133*, 1278; d) E. Ruiz-Hernandez, A. Baeza, M. Vallet-Regi, *ACS Nano* **2011**, *5*, 1259; e) A. Schlossbauer, S. Warncke, J. Kecht, A. Manetto, T. Carell, T. Bein, *Angew. Chem. Int. Ed.* **2010**, *49*, 4734; f) C. Chen, J. Geng, F. Pu, X. Yang, J. Ren, X. Qu, *Angew. Chem. Int. Ed.* **2011**, *50*, 882.

[13] L. Wang, Y. Liu, W. Li, X. Jiang, Y. Ji, X. Wu, L. Xu, Y. Qiu, K. Zhao, T. Wei, Y. Li, Y. Zhao, C. Chen, *Nano Lett.* **2011**, *11*, 772.

[14] a) J. Kim, H. S. Kim, N. Lee, T. Kim, H. Kim, T. Yu, I. C. Song, W. K. Moon, T. Hyeon, *Angew. Chem. Int. Ed.* **2008**, *47*, 8438; b) C. Wu, Q. H. Xu, *Langmuir* **2009**, *25*, 9441.

[15] a) L. M. Liz-Marzan, M. Giersig, P. Mulvaney, *Langmuir* **1996**, *12*, 4329; b) N. Li, H. Wang, M. Xue, C. Chang, Z. Chen, L. Zhuo, B. Tang, *Chem. Commun.* **2012**, *48*, 2507.

[16] a) D. S. Seferos, A. E. Prigodich, D. A. Giljohann, P. C. Patel, C. A. Mirkin, *Nano Lett.* **2009**, *9*, 308; b) N. Li, C. Chang, W. Pan, B. Tang, *Angew. Chem. Int. Ed.* **2012**, *51*, 7426.